

Hubble parameter measurement constraints on the cosmological deceleration-acceleration transition redshift

Omer Farooq and Bharat Ratra

Department of Physics, Kansas State University, 116 Cardwell Hall, Manhattan, KS 66506, USA

omer@phys.ksu.edu, ratra@phys.ksu.edu

ABSTRACT

We compile a list of 28 independent measurements of the Hubble parameter between redshifts $0.07 \leq z \leq 2.3$ and use this to place constraints on model parameters of constant and time-evolving dark energy cosmologies. These $H(z)$ measurements by themselves require a currently accelerating cosmological expansion at about, or better than, 3σ confidence. The mean and standard deviation of the 6 best-fit model deceleration-acceleration transition redshifts (for the 3 cosmological models and 2 Hubble constant priors we consider) is $z_{\text{da}} = 0.74 \pm 0.05$, in good agreement with the recent Busca et al. (2012) determination of $z_{\text{da}} = 0.82 \pm 0.08$ based on 11 $H(z)$ measurements between redshifts $0.2 \leq z \leq 2.3$, almost entirely from BAO-like data.

1. Introduction

In the standard picture of cosmology, dark energy powers the current accelerating cosmological expansion but played a less significant role in the past when nonrelativistic (cold dark and baryonic) matter dominated and powered the then decelerating cosmological expansion.¹ It is of some interest to determine the redshift of the deceleration-acceleration

¹ For reviews of dark energy see Bolotin et al. (2011), Martin (2012), and references therein. The observed accelerating cosmological expansion has also be interpreted as indicating the need to modify general relativity. In this paper we assume that general relativity provides an adequate description of gravitation on cosmological length scales. For reviews of modified gravity see Bolotin et al. (2011), Capozziello & De Laurentis (2011), and references therein.

transition predicted to exist in dark energy cosmological models. There have been a number of attempts to do so, see, e.g., Lu et al. (2011a), Giotri et al. (2012), Lima et al. (2012), and references therein. However, until very recently, this has not been possible because there has not been much high-quality data at high enough redshift (i.e., for z above the transition redshift in standard dark energy cosmological models).

The recent Busca et al. (2012) detection of the baryon acoustic oscillation (BAO) peak at $z = 2.3$ in the Ly α forest has dramatically changed the situation by allowing for a high precision measurement of the Hubble parameter $H(z)$ at $z = 2.3$, well in the matter dominated epoch of the standard dark energy cosmological model. Busca et al. (2012) use this and 10 other $H(z)$ measurements, largely based on BAO-like data, and the Riess et al. (2011) HST determination of the Hubble constant, in the context of the standard Λ CDM cosmological model, to estimate a deceleration-acceleration transition redshift of $z_{\text{da}} = 0.82 \pm 0.08$.

In this paper we extend the analysis of Busca et al. (2012). We first compile a list of 28 independent $H(z)$ measurements.² We then use these 28 measurements to constrain cosmological parameters in 3 different dark energy models and establish that the models are a good fit to the data and that the data provide tight constraints on the model parameters. Finally we use the models to estimate the redshift of the deceleration-acceleration transition. Busca et al. (2012) have one measurement (of 11) above their estimated $z_{\text{da}} = 0.82$, while we have 9 of 28 above this (and 10 of 28 above our estimated redshift $z_{\text{da}} = 0.74$). Granted, the Busca et al. (2012) $z = 2.3$ measurement carries great weight because of the small, 3.6%, uncertainty, but 9 of our 10 high redshift measurements, from Simon et al. (2005), Stern et al. (2010), and Moresco et al. (2012), include 3 11%, 13%, and 14% measurements from Moresco et al. (2012) and 3 10% measurements from Simon et al. (2005), all 6 of which carry significant weight.

Dark energy, most simply thought of as a negative pressure substance, dominates the current cosmological energy budget. In this paper we consider 3 dark energy models.

The first one is the “standard” spatially-flat Λ CDM cosmological model (Peebles 1984). In this model a little over 70% of the current energy budget is dark energy (Einstein’s cosmological constant Λ), non-relativistic cold dark matter (CDM) being the next largest contributor (a little over 20%), followed by non-relativistic baryonic matter (about 5%). In

² It appears that some of the measurements listed in Table 2 of Busca et al. (2012) might not be independent. For instance, the Chuang & Wang (2012a) and the Xu et al. (2012b) determinations of $H(z = 0.35)$ listed in the table are both based on the use of Sloan Digital Sky Survey Data Release 7 measurements of luminous red galaxies.

the Λ CDM model the dark energy density is constant in time and does not vary in space. Λ CDM has a number of well-known puzzling features (see, e.g., Peebles & Ratra 2003).

These puzzles could be eased if the dark energy density is a slowly decreasing function of time (Ratra & Peebles 1988).³ In this paper we consider a slowly-evolving dark energy scalar field model as well as a time-varying dark energy parameterization.

In Λ CDM, time-independent dark energy density is modeled as a spatially homogeneous fluid with equation of state $p_\Lambda = -\rho_\Lambda$ where p_Λ and ρ_Λ are the fluid pressure and energy density. Much use has been made of a parametrization of slowly-decreasing dark energy density known as XCDM where dark energy is modeled as a spatially homogeneous fluid with equation of state $p_X = w_X\rho_X$. The equation of state parameter $w_X < -1/3$ is independent of time and p_X and ρ_X are the pressure and energy density of the X -fluid. When $w_X = -1$ the XCDM parameterization reduces to the complete and consistent Λ CDM model. For any other value of $w_X < -1/3$ the XCDM parameterization is incomplete as it cannot describe spatial inhomogeneities (see, e.g. Ratra 1991; Podariu & Ratra 2000). For computational simplicity, in the XCDM case we assume a spatially-flat cosmological model. The ϕ CDM model is the simplest, consistent and complete model of slowly-decreasing dark energy density (Ratra & Peebles 1988). Here dark energy is modeled as a scalar field, ϕ , with a gradually decreasing (in ϕ) potential energy density $V(\phi)$. In this paper we assume an inverse power-law potential energy density $V(\phi) \propto \phi^{-\alpha}$, where α is a nonnegative constant (Peebles & Ratra 1988). When $\alpha = 0$ the ϕ CDM model reduces to the corresponding Λ CDM case. For computational simplicity, we again only consider the spatially-flat cosmological case for ϕ CDM.

Many different data sets have been used to derive constraints on the 3 cosmological models we consider here.⁴ Of interest to us here are measurements of the Hubble parameter as a function of redshift (e.g., Jimenez et al. 2003; Samushia & Ratra 2006; Samushia et al. 2007; Sen & Scherrer 2008; Chen & Ratra 2011b; Duan et al. 2011; Aviles et al. 2012; Seikel et al. 2012). Table 1 lists 28 $H(z)$ measurements. We only include independent measurements of $H(z)$, listing only the most recent result from analyses of a given data set. The values in Table 1 have been determined using a number of different techniques; for details see the papers listed in the table caption. Table 1 is the largest set of independent $H(z)$ measurements

³ For recent discussions of time-varying dark energy models, see Gu et al. (2012), Basilakos et al. (2012), Xu et al. (2012a), Guendelman & Kaganovich (2012), and references therein.

⁴ See, e.g., Chae et al. (2004), Samushia & Ratra (2008), Lu et al. (2011b), Dantas et al. (2011), Cao et al. (2012), Chen & Ratra (2012), Jackson (2012), Campanelli et al. (2012), Poitras (2012), and references therein.

z	$H(z)$ (km s ⁻¹ Mpc ⁻¹)	σ_H (km s ⁻¹ Mpc ⁻¹)	Reference
0.070	69	19.6	5
0.100	69	12	1
0.120	68.6	26.2	5
0.170	83	8	1
0.179	75	4	3
0.199	75	5	3
0.200	72.9	29.6	5
0.270	77	14	1
0.280	88.8	36.6	5
0.350	76.3	5.6	7
0.352	83	14	3
0.400	95	17	1
0.440	82.6	7.8	6
0.480	97	62	2
0.593	104	13	3
0.600	87.9	6.1	6
0.680	92	8	3
0.730	97.3	7.0	6
0.781	105	12	3
0.875	125	17	3
0.880	90	40	2
0.900	117	23	1
1.037	154	20	3
1.300	168	17	1
1.430	177	18	1
1.530	140	14	1
1.750	202	40	1
2.300	224	8	4

Table 1: Hubble parameter versus redshift data. Last column reference numbers: 1. Simon et al. (2005), 2. Stern et al. (2010), 3. Moresco et al. (2012), 4. Busca et al. (2012), 5. Zhang et al. (2012), 6. Blake et al. (2012), 7. Chuang & Wang (2012b).

considered to date.

We first use these data to derive constraints on cosmological parameters of the 3 models described above. The constraints derived here are compatible with cosmological parameter constraints determined by other techniques. These constraints are more restrictive than those derived by Farooq & Ratra (2012) using the previous largest set of $H(z)$ measurements, as well as those derived from the recent SNIa data compilation of Suzuki et al. (2012). The $H(z)$ data considered here require accelerated cosmological expansion at the current epoch at about or more than 3σ confidence.

Our paper is organized as follows. In the next section we present constraints from the $H(z)$ data on cosmological parameters of the 3 models we consider, establish that the 3 models are very consistent with the $H(z)$ data, and use the models to estimate the redshift of the cosmological deceleration-acceleration transition. We conclude in Sec. 3.

2. Constraints from the $H(z)$ data

Following Farooq et al. (2013), we use the 28 independent $H(z)$ data points listed in Table 1 to constrain cosmological model parameters. The observational data consist of measurements of the Hubble parameter $H_{\text{obs}}(z_i)$ at redshifts z_i , with the corresponding one standard deviation uncertainties σ_i . To constrain cosmological parameters \mathbf{p} of the models of interest we build the posterior likelihood function $\mathcal{L}_H(\mathbf{p})$ that depends only on the \mathbf{p} by integrating the product of $\exp(-\chi_H^2/2)$ and the H_0 prior likelihood function $\exp[-(H_0 - \bar{H}_0)^2/(2\sigma_{H_0}^2)]$, as in Eq. 18 of Farooq et al. (2013). We marginalize over the nuisance parameter H_0 using two different Gaussian priors with $\bar{H}_0 \pm \sigma_{H_0} = 68 \pm 2.8 \text{ km s}^{-1} \text{ Mpc}^{-1}$ (Chen et al. 2003; Chen & Ratra 2011a) and with $\bar{H}_0 \pm \sigma_{H_0} = 73.8 \pm 2.4 \text{ km s}^{-1} \text{ Mpc}^{-1}$ (Riess et al. 2011). As discussed there, the Hubble constant measurement uncertainty can significantly affect cosmological parameter estimation (for a recent example see, e.g., Calabrese et al. 2012). We determine the parameter values that maximize the likelihood function and find 1, 2, and 3 σ constraint contours by integrating the likelihood function, starting from the maximum and including 68.27 %, 95.45 %, and 99.73 % of the probability.

Figures 1–3 show the constraints from the $H(z)$ data for the three dark energy models we consider, and for the two different H_0 priors. In all 6 cases the $H(z)$ data of Table 1 require accelerated cosmological expansion at the current epoch, at, or better than, 3σ confidence. The previous largest $H(z)$ data set used, that in Farooq & Ratra (2012), required this accelerated expansion at, or better than, 2σ confidence. Comparing Figs. 1–3 here to Figs. 1–3 of Farooq & Ratra (2012), we see that in the Λ CDM and ϕ CDM cases the $H(z)$

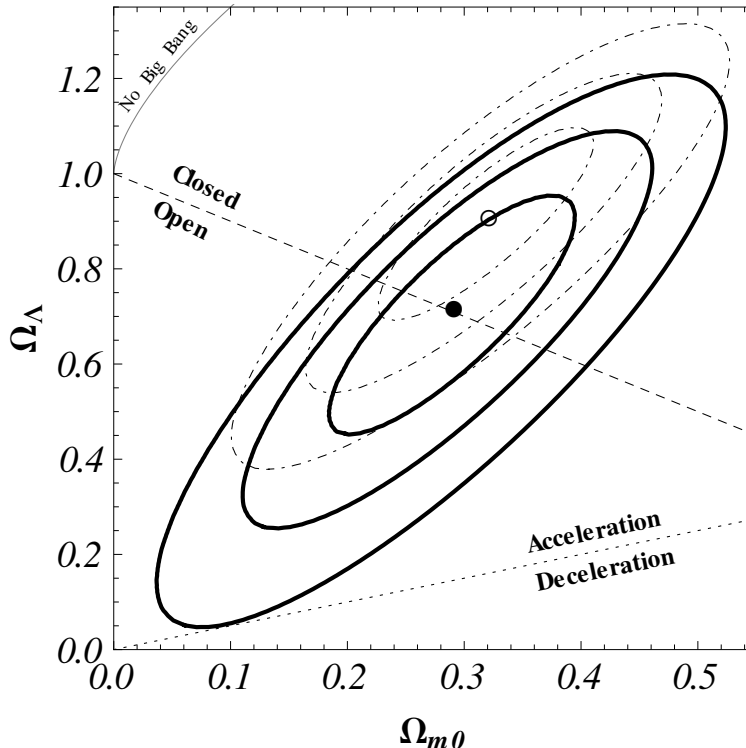


Fig. 1.— Solid [dot-dashed] lines show 1, 2, and 3 σ constraint contours for the Λ CDM model from the $H(z)$ data given in Table 1 for the prior $\bar{H}_0 \pm \sigma_{H_0} = 68 \pm 2.8 \text{ km s}^{-1} \text{ Mpc}^{-1}$ [$\bar{H}_0 \pm \sigma_{H_0} = 73.8 \pm 2.4 \text{ km s}^{-1} \text{ Mpc}^{-1}$]. The filled [empty] circle best-fit point is at $(\Omega_{m0}, \Omega_{\Lambda}) = (0.29, 0.72)$ [(0.32, 0.91)] with $\chi^2_{\min} = 18.24$ [19.30]. The dashed diagonal line corresponds to spatially-flat models, the dotted line demarcates zero-acceleration models, and the area in the upper left-hand corner is the region for which there is no big bang. The 2 σ intervals from the one-dimensional marginalized probability distributions are $0.15 \leq \Omega_{m0} \leq 0.42$, $0.35 \leq \Omega_{\Lambda} \leq 1.02$ [$0.20 \leq \Omega_{m0} \leq 0.44$, $0.62 \leq \Omega_{\Lambda} \leq 1.14$].

data we use in this paper significantly tightens up the constraints on w_X and α , but does not much affect the Ω_{m0} constraints. However, in the Λ CDM case the $H(z)$ data used here tightens up constraints on both Ω_{Λ} and Ω_{m0} .

As indicated by the χ^2_{\min} values listed in the captions of Figs. 1–3, all 6 best-fit models are very consistent with the $H(z)$ data listed in Table 1. It is straightforward to compute the cosmological deceleration-acceleration transition redshift in these cases. They are 0.706 [0.785], 0.695 [0.718], and 0.698 [0.817] for the Λ CDM, XCDM, and ϕ CDM models with prior $\bar{H}_0 \pm \sigma_{H_0} = 68 \pm 2.8 \text{ km s}^{-1} \text{ Mpc}^{-1}$ [$\bar{H}_0 \pm \sigma_{H_0} = 73.8 \pm 2.4 \text{ km s}^{-1} \text{ Mpc}^{-1}$]. The mean and standard deviation give $z_{\text{da}} = 0.74 \pm 0.05$, in good agreement with the recent Busca et al. (2012) determination of $z_{\text{da}} = 0.82 \pm 0.08$ based on less data, possibly not all independent.

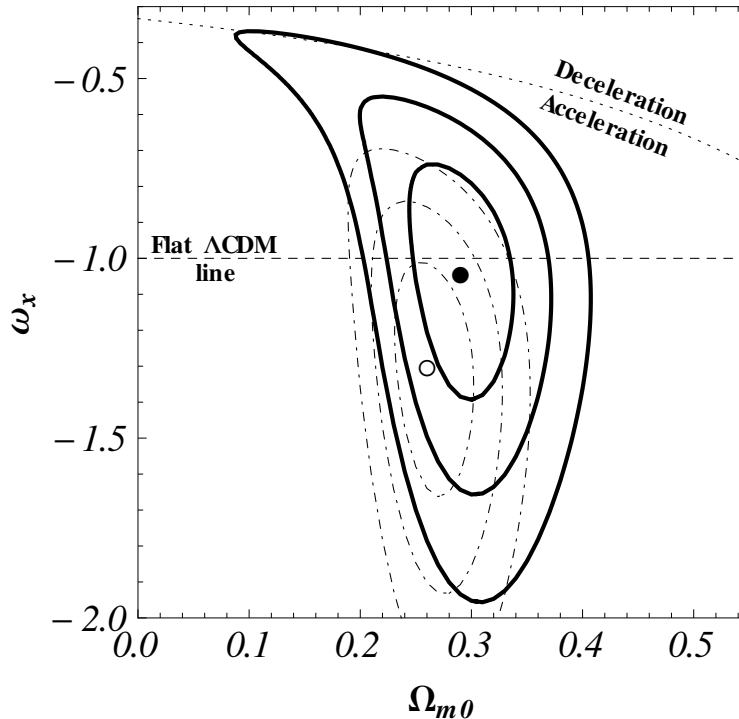


Fig. 2.— Solid [dot-dashed] lines show 1, 2, and 3 σ constraint contours for the XCDM parametrization from the $H(z)$ data given in Table 1 for the prior $\bar{H}_0 \pm \sigma_{H_0} = 68 \pm 2.8$ $\text{km s}^{-1} \text{Mpc}^{-1}$ [$\bar{H}_0 \pm \sigma_{H_0} = 73.8 \pm 2.4$ $\text{km s}^{-1} \text{Mpc}^{-1}$]. The filled [empty] circle is the best-fit point at $(\Omega_{m0}, \omega_X) = (0.29, -1.04)$ [(0.26, -1.30)] with $\chi^2_{\min} = 18.18$ [18.15]. The dashed horizontal line at $\omega_X = -1$ corresponds to spatially-flat Λ CDM models and the curved dotted line demarcates zero-acceleration models. The 2 σ intervals from the one-dimensional marginalized probability distributions are $0.23 \leq \Omega_{m0} \leq 0.35$, $-1.51 \leq \omega_X \leq -0.64$ [$0.22 \leq \Omega_{m0} \leq 0.31$, $-1.78 \leq \omega_X \leq -0.92$].

Figure 4 shows $H(z)/(1+z)$ data from Table 1 and the 6 best-fit model predictions as a function of redshift. The deceleration-acceleration transition is not impossible to discern in the data.

3. Conclusion

In summary, we have extended the analysis of Busca et al. (2012) to a larger independent set of 28 $H(z)$ measurements and determined the cosmological deceleration-acceleration transition redshift $z_{\text{da}} = 0.74 \pm 0.05$. These $H(z)$ data are well-described by all 6 best-fit models, and provide tight constraints on the model parameters. The $H(z)$ data require

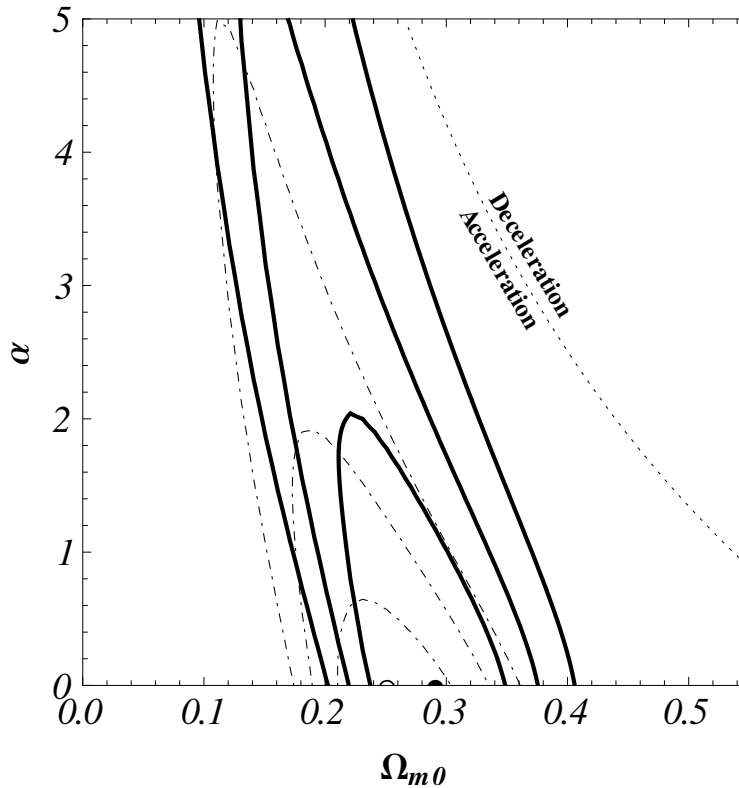


Fig. 3.— Solid [dot-dashed] lines show 1, 2, and 3 σ constraint contours for the ϕ CDM model from the $H(z)$ data given in Table 1 for the prior $\bar{H}_0 \pm \sigma_{H_0} = 68 \pm 2.8 \text{ km s}^{-1} \text{ Mpc}^{-1}$ [$\bar{H}_0 \pm \sigma_{H_0} = 73.8 \pm 2.4 \text{ km s}^{-1} \text{ Mpc}^{-1}$]. The filled [empty] circle best-fit point is at $(\Omega_{m0}, \alpha) = (0.29, 0)$ [(0.25, 0)] with $\chi^2_{\text{min}} = 18.24$ [20.64]. The horizontal axis at $\alpha = 0$ corresponds to spatially-flat Λ CDM models and the curved dotted line demarcates zero-acceleration models. The 2 σ intervals from the one-dimensional marginalized probability distributions are $0.17 \leq \Omega_{m0} \leq 0.34$, $\alpha \leq 2.2$ [$0.16 \leq \Omega_{m0} \leq 0.34$, $\alpha \leq 0.7$].

accelerated cosmological expansion at the current epoch, and are consistent with the decelerated cosmological expansion at earlier times predicted and required in standard dark energy models. While the standard spatially-flat Λ CDM model is very consistent with the $H(z)$ data, current $H(z)$ data are not able to rule out slowly evolving dark energy. More, and better quality, data are needed to better discriminate between constant and slowly-evolving dark energy density; these data are likely to soon be in hand.

We thank Mikhail Makouski and Data Mania for useful discussions and helpful advice. This work was supported in part by DOE grant DEFG03-99EP41093 and NSF grant AST-1109275.

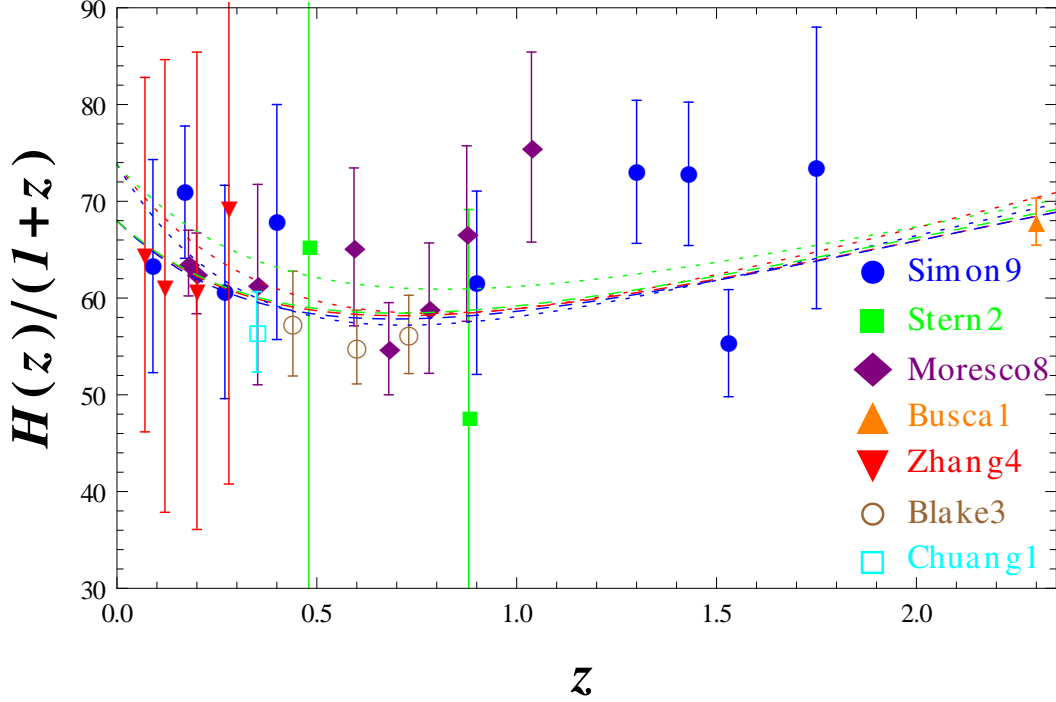


Fig. 4.— $H(z)/(1+z)$ data (28 points) and model predictions (lines for 6 best-fit models) as a function of redshift. The dashed [dotted] lines are for the prior $\bar{H}_0 \pm \sigma_{H_0} = 68 \pm 2.8 \text{ km s}^{-1} \text{ Mpc}^{-1}$ [$\bar{H}_0 \pm \sigma_{H_0} = 73.8 \pm 2.4 \text{ km s}^{-1} \text{ Mpc}^{-1}$], with red, blue, and green lines corresponding to the Λ CDM, XCDM, and ϕ CDM cases.

REFERENCES

- Aviles, A., et al. 2012, arXiv:1204.2007 [astro-ph.CO]
- Basilakos, S., Polarski, D., & Solà, J. 2012, arXiv:1204.4806 [astro-ph.CO]
- Blake, C., et al. 2012, MNRAS, 425, 405
- Bolotin, Yu. L., Lemets, O. A., & Yerokhin, D. A. 2011, arXiv:1108.0203 [astro-ph.CO]
- Busca, N. G., et al. 2012, arXiv:1211.2616
- Calabrese, E., et al. 2012, Phys. Rev. D, 86, 043520
- Campanelli, L., et al. 2012, Eur. Phys. J. C, 72, 2218
- Cao, S., et al. 2012, J. Cosmology Astropart. Phys., 1203, 016
- Capozziello, S., & De Laurentis, M. 2011, Phys. Rept., 509, 167

- Chae, K.-H., et al. 2004, *ApJ*, 607, L71
- Chen, G., Gott, J. R., & Ratra, B. 2003, *PASP*, 115, 1269
- Chen, G., & Ratra, B. 2011a, *PASP*, 123, 1127
- Chen, Y., & Ratra, B. 2011b, *Phys. Lett. B*, 703, 406
- Chen, Y., & Ratra, B. 2012, *A&A*, 543, A104
- Chuang, C. H., & Wang, Y., 2012a, *MNRAS*, 426, 226
- Chuang, C. H., & Wang, Y., 2012b, arXiv:1209.0210 [astro-ph.CO]
- Dantas, M. A., et al. 2011, *Phys. Lett. B*, 699, 239
- Duan, X., Li, Y., & Gao, C. 2011, arXiv:1111.3423 [astro-ph.CO]
- Farooq, O., Mania, D., & Ratra, B. 2013, *ApJ*, in press, arXiv:1211.4253 [astro-ph.CO]
- Farooq, O., & Ratra, B. 2012, arXiv:1212.4264 [astro-ph.CO]
- Giostri, R., et al. 2012, *J. Cosmology Astropart. Phys.*, 1203, 027
- Gu, J. A., Lee, C.-C., & Geng, C.-Q. 2012, arXiv:1204.4048 [astro-ph.CO]
- Guendelman, E. I., & Kaganovich, A. B. 2012, arXiv:1208.2132 [gr-qc]
- Jackson, J. C. 2012, arXiv:1207.0697 [astro-ph.CO]
- Jimenez, R., et al. 2003, *ApJ*, 593, 622
- Lima, J. A. S., et al. 2012, arXiv:1205.4688 [astro-ph.CO]
- Lu, J., Xu, L., & Liu, M. 2011a, *Phys. Lett. B*, 699, 246
- Lu, J., et al. 2011b, *Eur. Phys. J. C*, 71, 1800
- Martin, J. 2012, *C. R. Physique*, 13, 566
- Moresco, M., et al. 2012, *J. Cosmology Astropart. Phys.*, 1208, 006
- Peebles, P. J. E. 1984, *ApJ*, 284, 439
- Peebles, P. J. E., & Ratra, B. 1988, *ApJ*, 325, L17
- Peebles, P. J. E., & Ratra, B. 2003, *Rev. Mod. Phys.*, 75, 559

- Percival, W. J., et al. 2010, MNRAS, 401, 2148
- Podariu, S., & Ratra, B. 2000, ApJ, 532, 109
- Poitras, V. 2012, J. Cosmology Astropart. Phys., 1206, 039
- Ratra, B. 1991, Phys. Rev. D, 43, 3802
- Ratra, B., & Peebles, P. J. E. 1988, Phys. Rev. D, 37, 3406
- Riess, A. G., et al. 2011, ApJ, 730, 119
- Samushia, L., Chen, G., & Ratra, B. 2007, arXiv:0706.1963 [astro-ph]
- Samushia, L., & Ratra, B. 2006, ApJ, 650, L5
- Samushia, L., & Ratra, B. 2008, ApJ, 680, L1
- Seikel, M., et al. 2012, Phys. Rev. D, 86, 083001
- Sen, A. A., & Scherrer, R. J. 2008, Phys. Lett. B, 659, 457
- Simon, J., Verde, L., & Jimenez, R. 2005, Phys. Rev. D, 71, 123001
- Stern, D., et al. 2010, J. Cosmology Astropart. Phys., 1002, 008
- Suzuki, N., et al. 2012, ApJ, 746, 85
- Xu, L., Wang, Y., & Noh, H. 2012a, Eur. Phys. J. C, 72, 1931
- Xu, X., et al. 2012b, arXiv:1206.6732 [astro-ph.CO]
- Zhang, C., et al. 2012, arXiv:1207.4541 [astro-ph.CO]